

Salgımlar Neden Dalgalar Halinde İlerler?

Ayşe PEKER DOBIE¹, Semra AHMETOLAN², Ayşe Hümeysra BİLGE³, Ali DEMİRCİ^{4*}

^{1,2,4} İstanbul Teknik Üniversitesi, Fen- Edebiyat Fakültesi, Matematik Bölümü, İstanbul

³ Kadir Has Üniversitesi, Mühendislik ve Doğa Bilimleri Fakültesi, Endüstri Mühendisliği Bölümü, İstanbul

¹<https://orcid.org/0000-0002-5228-7694>

²<https://orcid.org/0000-0003-1003-7918>

³<https://orcid.org/0000-0002-6043-0833>

⁴<https://orcid.org/0000-0001-9780-0132>

*Sorumlu yazar: demircial@itu.edu.tr

Araştırma Makalesi

Makale Tarihiçesi:

Geliş tarihi: 31.07.2024

Kabul tarihi: 30.01.2025

Online Yayınlanma: 12.03.2025

Anahtar Kelimeler:

İspanyol gribi

COVID-19

Epidemi dalgaları

SIR modeli

Temel üreme sayısı

Temas oranı

ÖZ

“İspanyol Gribi” salgınının, 1918-1919 yılları arasında, 18 ay süre içinde, üç dalga şeklinde ilerlediği bilinmektedir. Benzer şekilde COVID-19 pandemisi de 2019-2021 yılları arasında dalgalar halinde yayılım karakteri göstermiş olup, bu salgın için virüs varyantlarına dair veriler detaylı bir şekilde belgelenmiştir. Bu çalışmada, bu iki pandemiye ait veriler ışığında, birden fazla salgın dalgasının ortaya çıkmasına neden olan faktörler, Korunmasız (S)-Enfekte (I)-Bulaşıcı Olmayan (R), (SIR) salgın modeli temel alınarak incelenmiştir. Bu faktörler arasında; mevsimsel değişiklikler, kontrol önlemlerinin gevşetilmesi ve yeni varyantlar öne çıkmaktadır. Yeni bir varyantın ortaya çıkması yeni bir salgın olarak değerlendirilebilmektedir. Bir salgın dalgasının sona ermesiyle, kısıtlayıcı tedbirlerin gevşetilmesi, önceden korunan bireylerin yeniden Korunmasız (S) grubuna dahil olmasına neden olabilmektedir. Kısıtlamaların kaldırılması ayrıca, toplum içerisindeki etkileşimlerin artmasına ve virüsün bulaşma oranını ifade eden temel üreme sayısının (R_0) yükselmesine etki edebilmektedir. SIR modeli kullanılarak bu çalışma kapsamında yapılan simülasyonlar sonucunda, yayılma davranışını belirleyen etmenler içerisinde yeni bir varyantın ortaya çıkışının baskın faktör olduğu değerlendirilmiştir.

Why Do Epidemics Evolve in Waves?

Research Article

Article History:

Received: 31.07.2024

Accepted: 30.01.2025

Published online: 12.03.2025

Keywords:

Spanish flu

COVID-19

Epidemic waves

SIR model

Basic reproduction number

Contact rate

ABSTRACT

Multiple epidemic waves have been observed during the “Spanish Flu” (1918-1919) and the COVID-19 (2019-2021) pandemics. The “Spanish Flu” pandemic, characterized by the H1N1 viral strain, was a severe and well-documented pandemic that manifested itself in three distinct epidemic waves spanning a period of 18 months. The COVID-19 pandemic has also been characterized by multiple epidemic waves and its data also include information on the variants of the ancestor virus. In this study, potential factors contributing to the occurrence of multiple waves are discussed by employing the Susceptible- Infected- Removed SIR model. These factors may include seasonality effects and relaxation of control measures. The introduction of a new variant of a pathogen can initiate a new wave, representing a distinct epidemic event. Also, at the end of an epidemic wave, the relaxation of restrictions allows previously protected individuals to re-enter the susceptible population, leading to an increase in susceptible individuals (S). Finally, the easing of restrictions promotes higher interconnections within the susceptible population, increasing the basic reproduction number (R_0). By observing the

simulations using the Susceptible-Infected-Removed model, we can conclude that the introduction of a new variant seems to be more dominant among causes leading to a new wave.

To Cite: Peker Dobie A., Ahmetolan S., Bilge AH., Demirci A. Why Do Epidemics Evolve in Waves. *Osmaniye Korkut Ata Üniversitesi Fen Bilimleri Enstitüsü Dergisi* 2025; 8(2): 929-941.

1. Introduction

The Susceptible-Infected-Removed (SIR) and Susceptible-Exposed-Infected-Removed (SEIR) models, initially proposed by Kermack and McKendrick (Kermack and McKendrick, 1927; Hethcote, 1976) in 1927, serve as mathematical frameworks to describe the spread of epidemics within a population. In these models, individuals are categorized into different compartments based on their susceptibility to the disease and their infectivity status. The SIR model consists of three compartments: Susceptible (S), Infected (I), and Removed (R), representing individuals without immunity, infected individuals capable of transmitting the disease to group S with recovery after a period T, and individuals who have either recovered with permanent immunity or died, respectively. The SEIR model expands upon the SIR model by introducing an additional Exposed (E) compartment, which represents individuals in the incubation period of the disease before becoming infectious, with duration T_E . The differential equations governing the models defined by equations (1) and (2), respectively, describe the rates of change for each compartment over time

$$S' = -\beta SI, \quad I' = \beta SI - \eta I, \quad R' = \eta I, \quad (1)$$

$$S' = -\beta SI, \quad E' = \beta SI - \varepsilon E, \quad I' = \varepsilon E - \eta I, \quad R' = \eta I. \quad (2)$$

Here, β is the transmission coefficient, η represents the recovery rate which is the inverse of the infection period T, and ε , the inverse of the incubation period T_E represents the rate of progression from the exposed state to the infected state. These models provide a simplified representation of epidemic dynamics, and can be useful in analyzing and predicting the spread of diseases within populations based on various epidemiological parameters.

In both models, the ratio β/η is referred to as the Basic Reproduction Number denoted by R_0 . The Basic Reproduction Number serves as a crucial parameter that determines the final proportion of removed individuals, R_f , thereby influencing the overall burden of an epidemic. R_0 is the product of the contact rate, the virus's virulence and the duration of the infectious period. Variants with different virulence and infection periods, as well as seasonality effects and behavioral changes, can lead to variations in R_0 . However, barring such changes, it remains constant.

Childhood diseases are typical examples of epidemics obeying SIR models with population dynamics. These models allow almost periodic wave structures, attributed to the integration of newborns into the susceptible population. In the absence of population dynamics, the solutions of the basic SIR and SEIR models (equations (1) and (2), respectively) exhibit a singular wave of epidemic outbreaks. For seasonal influenza types of diseases, as the duration of the epidemic is relatively short compared to the timespan of population dynamics, models assuming a constant population provide valid insights in such cases.

Any disease conferring permanent immunity without population dynamics would ordinarily result in a single epidemic wave. Nevertheless, major historical pandemics have been characterized by a succession of waves. In models characterized by constant parameters and the absence of population dynamics, the emergence of a new epidemic wave may be ascribed to various factors such as the appearance of a novel variant, an upsurge in the susceptible population, or an increase in the Basic Reproduction Number, as examined in section 2. We explore the effects of changes in these parameters in section 3 by simulating scenarios involving increases in the number of susceptible individuals and increases in R_0 . The outcomes of these simulations reveal that the appearance of a new wave requires substantial increments in either of these parameters, thereby suggesting that the resurgence of a new wave is more likely to be triggered by the appearance of a novel variant.

Multiple epidemic waves have been discerned during the “Spanish Flu” (1918-1919) and the ongoing COVID-19 (2019-2021) pandemics. The “Spanish Flu” pandemic (Taubenberger and Morens, 2006), characterized by the H1N1 viral strain, was a severe and well-documented pandemic that manifested itself in three distinct epidemic waves spanning 18 months. Conversely, the H1N1 influenza pandemic of 2009 exhibited a predominantly unimodal pattern (Tizzoni et al., 2012) between October 2009 and May 2010, if one excludes the initial propagation observed during the summer of 2009. Furthermore, a multi-wave pattern has also been observed in the spread of COVID-19 from 2019 to 2022 (Xu et al., 2020; Lengfeld, 2021; Ghosh and Ghosh, 2022; Singh and Gupta, 2022; Perakis et al., 2023).

Below, we review recent works on the underlying mechanisms for manifesting multiple epidemic waves. Within a study (Perakis et. al., 2023), a comprehensive investigation was undertaken to explore the influence of regulations and alterations in human behavior on the inception of epidemic waves for COVID-19. Employing a model characterized by piecewise constant parameters, the authors sought to construct a stochastic framework for discerning the temporal transitions, with the primary objective of identifying the emergence of an epidemic wave from data.

In another research (Ghosh and Ghosh, 2022) the authors consider the potential loss of immunity after a time delay and the emergence of new variants to investigate the occurrence of multiple waves of COVID-19 in India. It should be noted that it is important to differentiate between the loss of immunity to a specific strain and the emergence of a new variant as a distinct strain. The latter scenario corresponds to seasonal epidemics, such as those observed annually for influenza, which are attributed to the appearance of novel strains. In contrast, diseases like malaria adhere to the Susceptible-Infected-Susceptible (SIS) model, where individuals regain susceptibility at the end of the infectious period. We note that the SIS model yields a series of periodic waves with the same amplitude, thus it is inappropriate for explaining the succession of multiple waves with diminishing amplitudes, as observed in historical epidemics.

The phenomenon of partial loss of immunity has been investigated in the context of COVID-19, particularly data from Wuhan, China (Langfeld, 2021), until April 2020. The model employed in this study demonstrates agreement with the observed data but does not account for the potential impact of

new variants. In a separate investigation (Xu et. al., 2020) multiple outbreaks are examined, incorporating heterogeneities in the pathogen, host characteristics, and environmental conditions. This research highlights the possibility of multiple waves based on these variabilities. Similarly, Singh and Gupta adopt an SIR model with variable parameters to capture the data about distinct waves (Singh and Gupta, 2022). In contrast, our approach follows a different trajectory, employing the SIR model with constant parameters but over shorter time periods, aligning more closely with the study in (Perakis et. al., 2023).

2. Material and Methods

In this section, we discuss potential factors contributing to the occurrence of multiple waves by employing the SIR model as a framework to investigate the effects of changes in the parameters. To observe these effects, the SIR model (1) is numerically solved using the fourth order Runge- Kutta method with appropriate initial conditions. Corresponding results are presented in Figures 2-4, accompanied by the necessary discussions. Furthermore, we present simulations aimed at quantifying these effects. The emergence of successive waves can be explained through the following arguments:

1) Novel variant: The introduction of a novel variant may give rise to a new wave, effectively representing a distinct epidemic event. In technical terms, individuals in the R compartment should be transferred to the S department; without any change in the total population size.

2) Increase in S and in the total population size: Following the culmination of an epidemic wave, the relaxation of restrictions allows individuals who diligently safeguarded themselves and thus were not part of the susceptible population to re-enter this category. Consequently, the susceptible population S experiences an increase that increases the total population size.

3) Increase in R_0 with constant population size: Upon the conclusion of an epidemic wave, the easing of restrictions facilitates heightened interconnections within the susceptible population. As a result, the contact rate and hence R_0 increase, while the total population size remains constant.

We will now discuss conditions ensuring resurging of a new epidemic wave, based on arguments 1-3.

We recall that in equation (1), the sum of the right-hand sides is zero, hence we can assume $S(t)+I(t)+R(t)=1$. As time goes to infinity, $I(t)$ approaches zero, hence we may state that the final value of I is zero, and the final values of S and R, denoted by S_f and R_f satisfy the relation $S_f = 1 - R_f$. Then, from equation (1), we use the chain rule and normalization conditions, and obtain the relation below between R_0 and the final values R_f and S_f

$$R_0 = -\frac{\ln(1 - R_f)}{R_f} = -\frac{\ln S_f}{1 - S_f}. \quad (3)$$

We use the relation above to plot R_f as a function of R_0 in Figure 1 where blue and green curves represent respectively the final proportion of susceptible individuals, S_f , and the proportion of susceptible individuals at the peak of the epidemic wave, S_m .

We note that the evaluation of S_f from equation (3) is a numerical procedure. For example, when R_0 equals 2, then S_f is determined as 0.203. On the other hand, S_m is expressed in terms of R_0 as $S_m = 1/R_0$, because $I(t)$ attains its maximum when its derivative is zero, corresponding to $S_m = \eta/\beta$ if $S(t)$ lies above the curve $S_m(R_0)$, then $I(t)$ is increasing; otherwise it is decreasing. In the falling phase of the epidemic, $S(t)$ lies between the blue and green curves. Therefore, if we expect a resurgence of a new wave at the falling phase of an epidemic, the pair (R_0, S) should move above the green curve $S_m(R_0)$. This can be achieved by an increase in R_0 , or in S , or both.

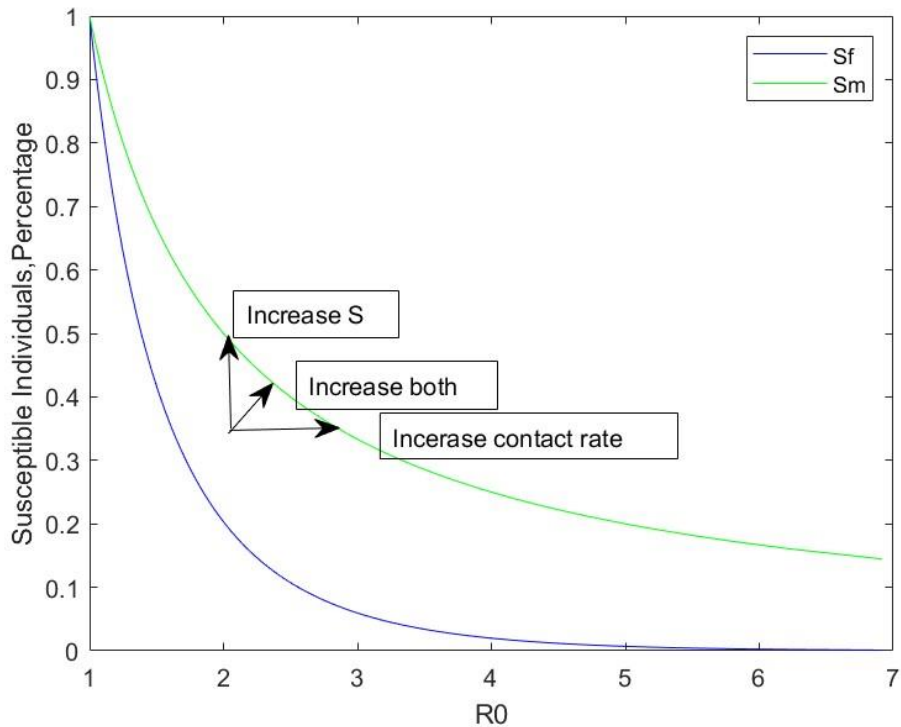


Figure 1. S_f as a function of R_0 (blue curve) and S_m as a function of R_0 (green curve).

We will now discuss the dynamics of the appearance of a new wave due to the causes 1-3.

-Case 1, Novel Variant: If a new variant emerges while the total population size remains constant (case 1), the proportion of susceptible individuals can potentially rise to 1. Furthermore, if R_0 for each new variant is the same, we would have a succession of epidemic waves with equal amplitude. If R_0 for successive variants decreases or increases, we expect a similar behavior in the amplitude of the epidemic waves.

A decrease in the amplitude of upcoming waves may also be due to the following fact: it is possible that some individuals who previously contracted the disease and acquired immunity during the initial wave exhibit some level of protection against the new strain. Consequently, a certain proportion of the individuals in the R department may have immunity to the new strain, and the proportion of susceptible individuals is lower at the beginning of the appearance of the new strain. Thus, despite the immunity acquired during the initial wave, if the sudden increase in $S(t)$ is substantial enough to move (R_0, S)

above the $S_m(R_0)$ curve, it would lead to a new wave. We illustrate this situation in Figure 2, where $R_0=1.5$ for both variants, the infection period T is 10, and it is assumed that 20% of the removed individuals still have immunity with respect to the new variant.

-Case 2, Increase in S and in the total population size: Even without the introduction of a new variant, the occurrence of a new epidemic wave is still possible if the proportion of susceptible individuals exceeds the threshold value $S_m = 1/R_0$, either due to an increase in R_0 or in S . An alternative scenario (case 2) entails an increase in the proportion of susceptible individuals following the cessation of an epidemic wave. This phenomenon may transpire when a specific fraction of the population, previously adhering to stringent isolation measures, discontinues their isolation and consequently transitions into the susceptible group. This leads to a vertical shift of a point on the blue curve, up towards the $1/R_0$ curve. Once again, if the change is substantial enough to end up to the left of the $1/R_0$ curve, it instigates the onset of a fresh epidemic wave.

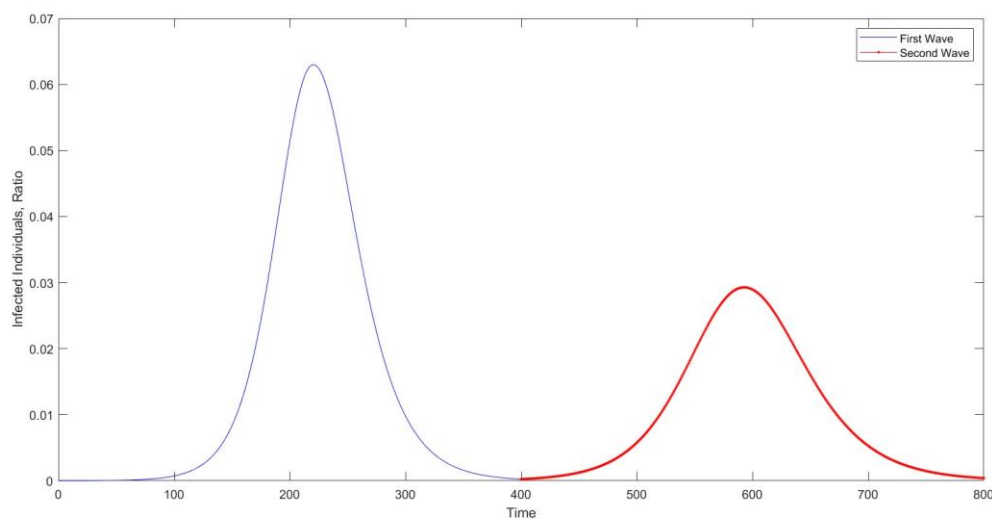


Figure 2. Resurge of a new epidemic wave by the introduction of a new variant, when $R_0=1.5$ for both variants and $T=10$. 20% of the removed individuals is assumed to have immunity with respect to the new variant.

In Figure 3, we present simulations for case 2 with typical parameter values. We consider the cases where $R_0=1.5$ and $R_0=2$. The ratio of the total population that has safeguarded themselves at the initial phase is taken as $2/3$ and $1/2$. In simulations, these people are added to the S group at the end of the first wave.

Even though we observe a second wave for each case, it is significant only in the extreme case where $2/3$ of the population has been in strict confinement during the whole duration of the first wave.

-Case 3, Increase in R_0 with constant population size: We recall that R_0 is the product of the virulence of the infection (v), the duration of the infectious period (T) and the contact rate (C), i.e.,

$$R_0 = v T C. \tag{4}$$

While ν and T are invariant in the absence of mutations, the contact rate may change. A rise in the contact rate, thus increasing R_0 (case 3), horizontally shifts a point along the blue curve towards the green curve. If the increase in the contact rate is substantial enough to position the point to the right of the $1/R_0$ curve (green curve), then the slope of $I(t)$ becomes positive, signaling the initiation of a new epidemic.

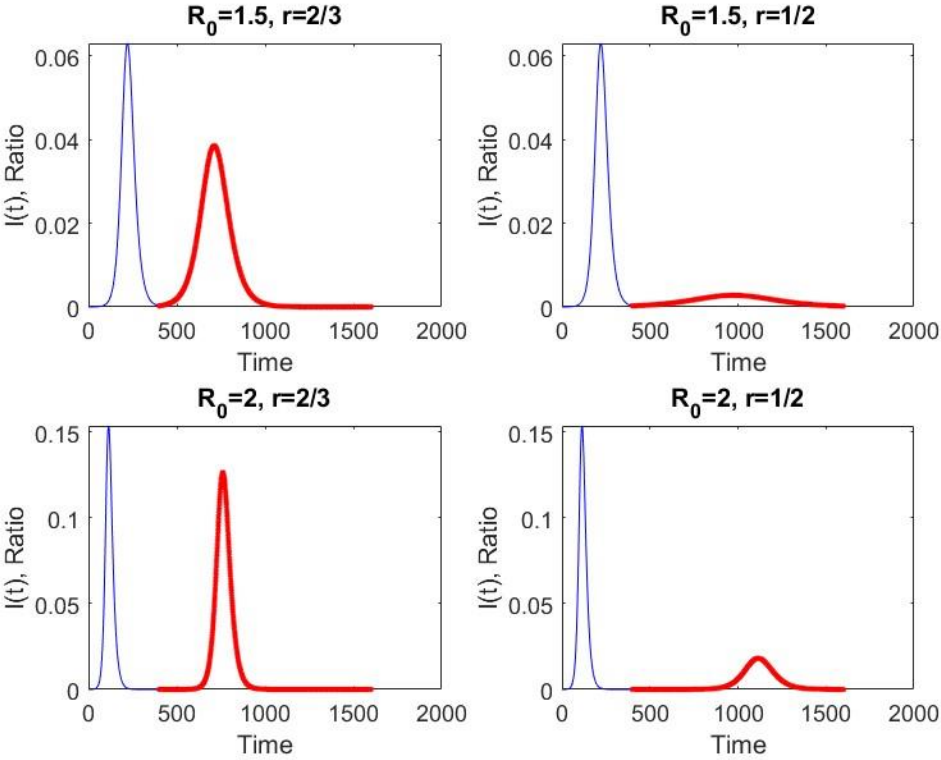


Figure 3. First and second waves corresponding to cases where proportions $r=2/3$ and $r=1/2$ of the population have safeguarded themselves during the first wave, for $R_0=1.5$ and $R_0=2$.

In Figure 4, we present typical situations corresponding to an increase in R_0 at a time at which the rate of change of the number of infectious individuals starts decreasing. This corresponds to release of restrictions towards the end of the epidemic wave and to a possible increase in the contact rate.

In Figure 4, we selected parameter values that lead to an observable second wave. For example, for $R_0=2$, initially, increases to 2.5 and 3.0 didn't result in a new wave. Furthermore, increases in R_0 chosen as 0.5 and 1 may not be realized by an increase in the contact rate in realistic situations.

We note that if the end of the epidemic wave coincides with the beginning of summer, the increase in the contact rate may be compensated by the decreased virulence, and there is no new wave. But if it ends at the beginning of the new flu season unless strict restrictions are imposed, a new wave can appear, even in the absence of a new variant.

3. Results and Discussion

The occurrence of multiple waves is a prominent characteristic observed in pandemics, including historical events such as the Spanish Flu and more recent outbreaks like the COVID-19 pandemic. Numerous studies (Xu et al., 2020; Lengfeld, 2021; Ghosh and Ghosh, 2022; Singh and Gupta, 2022; Perakis et al., 2023) have endeavored to elucidate the underlying factors contributing to the existence of multiple waves. In this section, we conduct a comprehensive literature review to examine the observations and findings pertaining to the occurrence of multiple waves in the Spanish flu pandemic of 1918, a notable example of a pandemic characterized by multiple waves that swept across the globe.

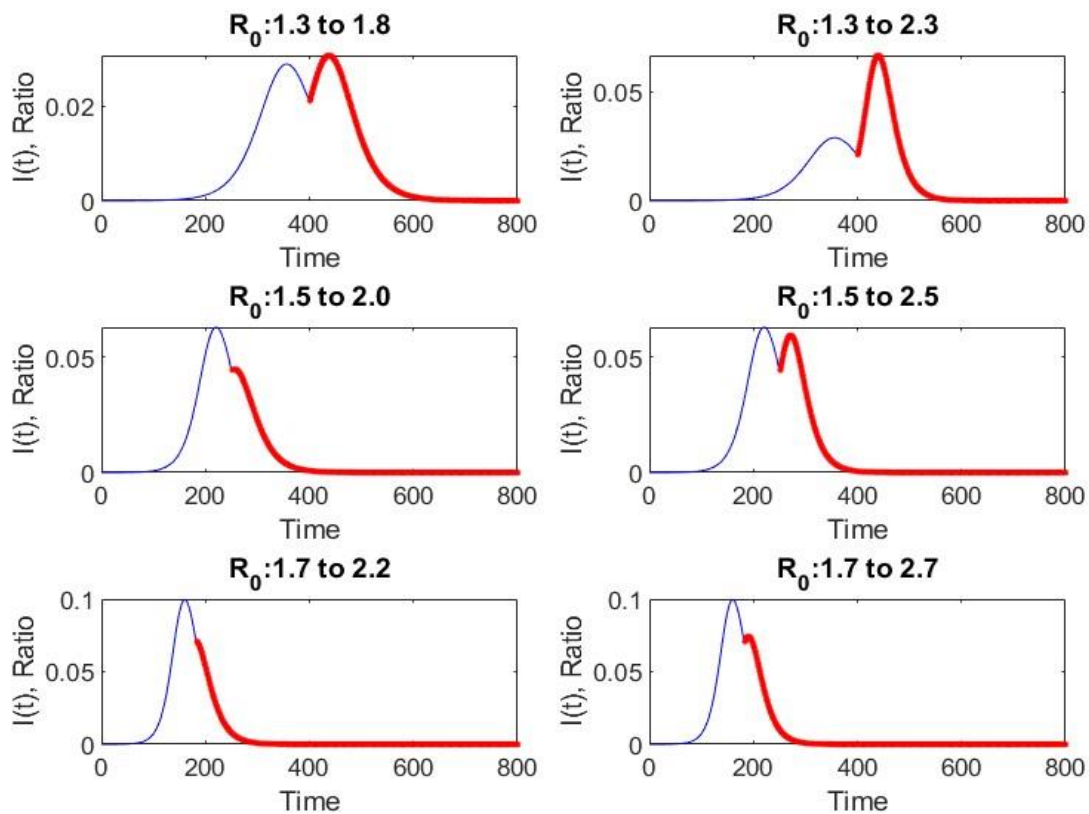


Figure 4. First and second waves corresponding to cases where the contact rate increases as indicated for $R_0=1.3, 1.5$ and 1.7 by amounts $\Delta R_0=0.5$ and 1 .

3.1. USA, St. Louis and Philadelphia data (the effect of contact rate)

Figure 5 portrays the death rate during the same Spanish flu pandemic in two distinct cities of the USA: Philadelphia and St. Louis (Hatchett, 2007). Notably, these two cities exhibited completely different patterns, attributed to the differing policies applied. A clear disparity can be observed in the curves, wherein the peak mortality rate in St. Louis amounted to merely one-eighth of the peak observed in the other city.

In Philadelphia, the state demonstrated a sluggish and hesitant response following the emergence of the first case. It was not until a significant parade took place on the 28th of September, 1918, with the participation of thousands of individuals, that the number of cases surged exponentially, resulting in a large-scale loss of life.

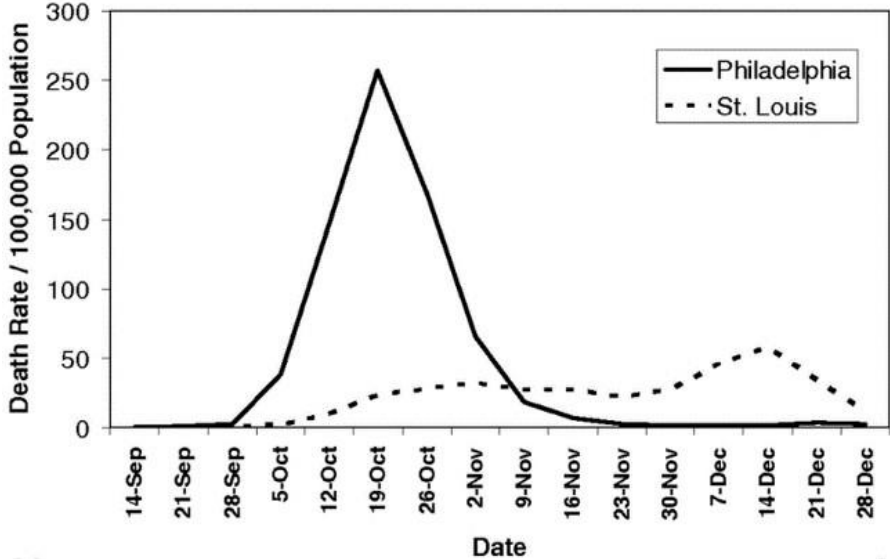


Figure 5. Weekly mortality data in Philadelphia and St. Louis, USA (Hatchett, 2007).

Conversely, in St. Louis, swift and stringent measures were implemented soon after the initial case, including the closure of schools and the prohibition of public gatherings. Consequently, the city successfully flattened the curve. However, when the restrictions were gradually lifted, cases began to rise again, particularly in December, 1918.

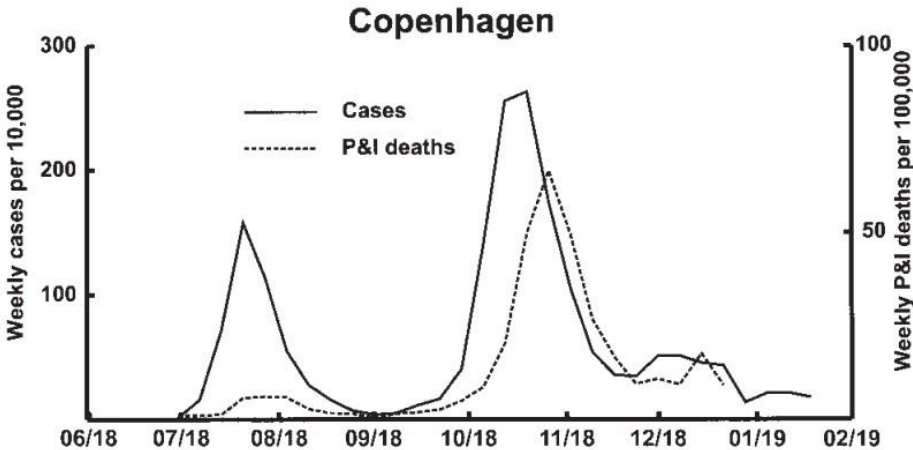


Figure 6. Weekly number of influenza cases and respiratory deaths (pneumonia and influenza) in Copenhagen, Denmark (Andreasen et al., 2008).

3.2. Denmark data (time shift between the peak of fatalities and the peak of infections)

Weekly cases recorded in Copenhagen during the Spanish flu pandemic (Andreasen et al., 2008) are shown in Figure 6. This data, characterized by a stronger second wave includes simultaneous records of cases and fatalities, and besides being an example of multiple waves, displays a time shift between the peak of cases and fatalities, a property that has been discussed in a previous work (Peker- Dobie et al., 2020).

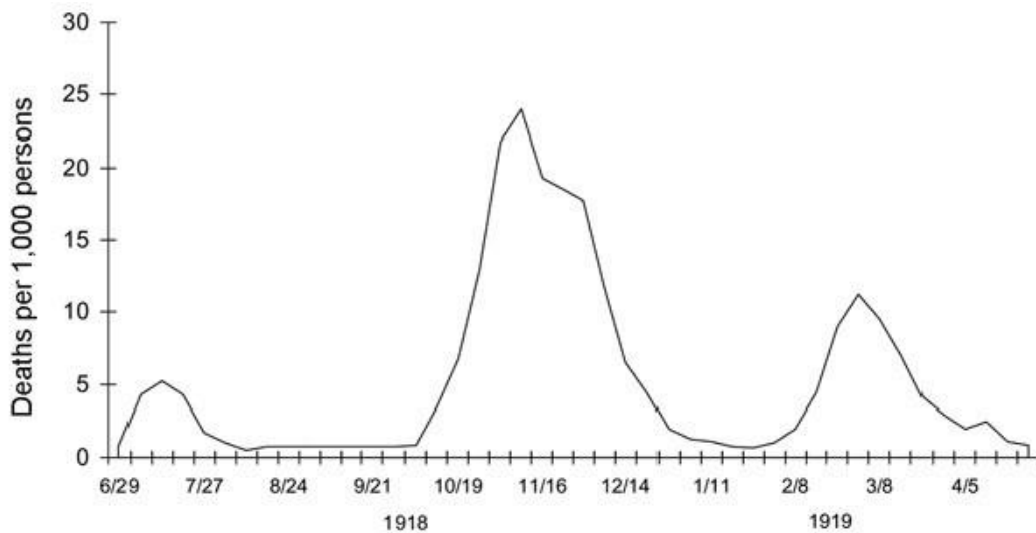


Figure 7. Historical data during the Spanish flu pandemic: Weekly number of deaths (pneumonia and influenza) in the United Kingdom (Jordan et al., 1927).

3.3. UK data (multiple waves)

Figure 7 depicts the monthly deaths in the United Kingdom (Jordan et al., 1927) within the time span of 29/6/1918 to 5/4/1919. This visual representation depicts the occurrence of three successive waves during the course of the pandemic, each exhibiting varying magnitudes. Notably, the first wave was relatively brief, whereas the second and third waves possessed similar longer durations, as indicated by their comparable widths.

3.4. Belfast and Dublin data (multiple waves)

In Figure 8, we observe the graphs depicting weekly death rates caused by the Spanish flu in two cities, Belfast and Dublin in Ireland. This information is credited to Dr. Patricia Marsh (Marsh, 2018). Notably, both cities experienced three waves of the pandemic, with each wave exhibiting approximately equal durations. Belfast displayed a higher peak during the first wave, whereas Dublin witnessed a higher peak during the third wave. The second waves in both cities appeared similar, albeit with a time shift.

3.5. General remarks

In these cases, the manifestation of epidemic waves appears to be associated with seasonality and the relaxation of control measures. It is important to note that during that time, sequence analyses were not available, thus limiting the ability to assess the role of viral variants in these waves.

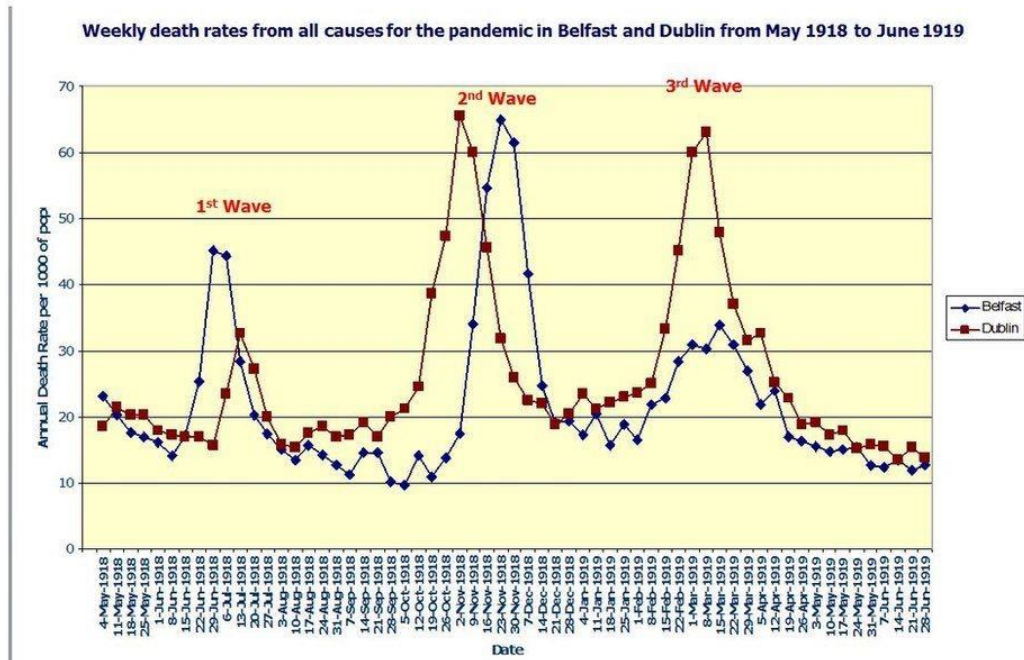


Figure 8. Historical data during the Spanish flu pandemic: Weekly death rates from all causes in Belfast and Dublin, Ireland (Marsh, 2018).

4. Conclusions

In this study, we explore the factors contributing to the occurrence of multiple waves in the course of an epidemic, using the SIR model as a framework. We investigate the effects of parameter changes and present simulations to quantify these effects. We propose that the emergence of successive waves can be explained by several factors. Firstly, the introduction of a new variant of the pathogen can initiate a new wave, representing a distinct epidemic event. Individuals who acquired immunity during the initial wave may have some level of protection against the new strain, affecting the ratio of removed individuals in the population. Secondly, after the end of an epidemic wave, the relaxation of restrictions allows previously protected individuals to re-enter the susceptible population, leading to an increase in susceptible individuals (S). Lastly, the easing of restrictions promotes higher interconnections within the susceptible population, resulting in an increase in the contact rate (R_0). Each of these factors contributes with varying degrees of influences to the birth of a new wave. Data from the 1918 Spanish flu is used to illustrate these effects.

The original model for the spread of epidemics, as proposed by Kermack and McKendrick (Kermack and McKendrick, 1927), is an integral equation, which reduces to the system of ordinary differential equations known as the SIR model under a special choice for the kernel. Actually, the SIR system in the

form of ordinary differential equations fails to replicate the delay between the peaks of infections and fatalities, as for the H1N1 epidemic in Istanbul (Peker-Dobie et al., 2020), but it is widely used in literature and it can be considered as a reasonable choice despite its simplicity. Linearized versions of the ODE SIR model, that are based on replacing the constant β in the model by a time varying, wave-like function described as the infectious force and those approaches that adopt a time varying basic reproduction number, are also common, but these variants of the SIR model fail to reproduce the inherent dynamics of the spread of the epidemics.

Models that involve population dynamics lead to wavelike behavior; these models are appropriate for childhood diseases and lead to a continuous succession of epidemic waves, hence they are not appropriate for explaining the finite wave sequence as observed for flu-type diseases. To the best of our knowledge, there is no comparable study that discusses the qualitative and quantitative reasons behind the wave-like progression of epidemics and their epidemiological causes.

Me varying, wave-like function described as the infectious force and those approaches that adopt a time varying basic reproduction number, are also common, but these variants of the SIR model fail to reproduce the inherent dynamics of the spread of the epidemics.

Models that involve population dynamics lead to wavelike behavior; these models are appropriate for childhood diseases and lead to a continuous succession of epidemic waves, hence they are not appropriate for explaining the finite wave sequence as observed for flu-type diseases. To the best of our knowledge, there is no comparable study that discusses the qualitative and quantitative reasons behind the wave-like progression of epidemics and their epidemiological causes.

Conflict of Interest

The authors declare that the research was conducted in the absence of any commercial or financial relationships that could be construed as a potential conflict of interest.

Authors' Contributions

All authors contributed to the article and approved the submitted version.

References

Andreasen V., Viboud C., Simonsen L. Epidemiologic characterization of the 1918 influenza pandemic

- summer wave in Copenhagen: implications for pandemic control strategies. *Journal of Infectious Diseases* 2008; 297(2): 270-278.
- Ghosh K., Ghosh AK. Study of COVID-19 epidemiological evolution in India with a multi-wave SIR model. *Nonlinear Dynamics* 2022; 109(1): 47-55.
- Hatchett RJ., Mecher CE., Lipsitch M. Public health interventions and epidemic intensity during the 1918 influenza Pandemic. *Proceedings of the National Academy of Science* 2007; 104(18): 7582-7587.
- Hethcote HW. Qualitative analyses of communicable disease models. *Mathematical Biosciences* 1976; 28(3-4): 335-356.
- Jordan EO. Epidemic influenza: A survey. 1927.
- Kermack WO., McKendrick AG. A contribution to the mathematical theory of epidemics. *Proceedings of the Royal Society of London. Series A, Containing papers of a Mathematical and Physical Character* 1927; 115(772): 700-721.
- Langfeld K. Dynamics of epidemic diseases without guaranteed immunity. *Journal of Mathematics in Industry* 2021; 11(1): 1-8.
- Marsh P. Spanish flu: How the 1918 pandemic hit Ulster and beyond. 2018, Accessed July 17, 2024, <https://www.bbc.com/news/uk-northern-ireland-46265074>
- Peker-Dobie A., Demirci A., Bilge AH., Ahmetolan S. On the time shift phenomena in epidemic models. *Frontiers in Physics* 2020; 8: 578455-578455.
- Perakis G., Singhvi D., Skali Lami O., Thayaparan L. COVID-19: A multiwave SIR-based model for learning waves. *Production and Operations Management* 2023; 32(5): 1471-1489.
- Singh P., Gupta A. Generalized SIR (GSIR) epidemic model: An improved framework for the predictive monitoring of COVID-19 pandemic. *ISA Transactions* 2022; 124: 31-40.
- Taubenberger JK., Morens DM. Influenza: the mother of all pandemics. *Revista Biomedica* 2006; 17(1): 69-79.
- Tizzoni M., Bajardi P., Poletto C., Ramasco JJ., Balcan D., Gonçalves B., Vespignani A. Real-time numerical forecast of global epidemic spreading: case study of 2009 A/H1N1pdm. *BMC Medicine* 2012; 10: 1-31.
- Xu B., Cai J., Chowell G., Xu B. Mechanistic modelling of multiple waves in an influenza epidemic of pandemic. *Journal of Theoretical Biology* 2020; 486: 110070-110070.